Reverse Engineering: Selective Sampling Acquisition Approach

REVERSE ENGINEERING: A SELECTIVE SAMPLING ACQUISITION APPROACH

E. Vezzetti

Dipartimento di Sistemi di Produzione Ed Economia dell'Azienda, Politecnico di Torino, Corso Duca degli Abruzzi 24, 10129,Torino, Italy, Ph: +39 011 5647294 Fax +39 0115647299

enrico.vezzetti@polito.it

Abstract

Creation of a CAD model from an hard model is something necessary for design modification, part replication or rapid prototyping and surface inspection. This is reverse engineering. Scientific literature presents many different approaches, even if, actually all the systems, mechanical (contact devices) and optical (non contact devices), work with constant acquisition pitches. This became a great deal in relation with the different object morphologies combinations that the same surface could show. Working in fact with a constant pitch on a free-form surface it is possible to struggle with an insufficient points cloud density, when the acquisition pitch would be a compromise between the complex and elementary features that describe the object to acquire, or with an excessive points cloud density, when the acquisition pitch represents the highest scanner resolution. Referring to this situation, this paper wants to propose, starting from a first raw acquisition, an automatic methodology, directly implemented on the acquisition device, for the selective individuation of surface zones which present sensible curvature. In this approach the curvature of the measured surfaces is analyzed by defining a threshold over which it is necessary to perform a deeper scansion of the surface. In the present paper a methodology for the definition of the threshold value based on the measurement system uncertainty is described. In the current description the method is applied to an algorithm for curvature analysis, but it could be extended to any other approaches. Furthermore, it will be demonstrated that this new methodology is simple to apply and can be easily automated directly in the control scanner software. In the end of the paper a practical example is described in order to give an experimental validation of the method.

Keywords: Reverse Engineering, Scanning Strategy, Geometric Morphology, Scanner 3D, Design

1. Introduction

Reverse engineering is the process of engineering backward to build a CAD model geometrically identical to an existing product. Subsequently, CAD models are used for manufacturing or other applications. An example application is where CAD models are unavailable, unusable, or insufficient for existing parts that must be duplicated or modified. There are many practical applications ranging from tool and die making to biomedical device design and manufacturing[1].

In order to better understand the topics aspects of this work, it is opportune to split the entire methodology in three main steps: point digitisation, segmentation and surface modelling. Focusing the attention on "point digitisation" and "surface modelling", it is necessary to highlight some relevant problems associated to the sampling strategy [2].

The surface point digitisation was normally developed with a manual process often time consuming and tedious, especially working with complex free-forms. Some commercial systems has automated this process by scanning the surface across a rectangular patch with a fixed scanning pitch. However, this method tends to pick up redundant points in relatively flat surface regions, and working with contact systems this asks a long acquisition time. The technological evolution of the acquisition devices has driven to the possibility to employ fast non contact digitisers, such as laser range finders, stereo image detectors, moiré interferometers and structured lighting devices, that can scan dense measurement data in a relatively short time. Even if this could be considered an attractive solution for the problem of scanning strategy choice, the obtained results are not always guaranteed in term of measurements accuracy. In fact, if the surface is complex and a very accurate model is required, the use of non contact acquisition device does not always represent the optimal solution [3] and the presence of very crowd points clouds, generated from the non contact devices, obliges to perform a strong data manipulation and filtering in order to lighten the successive elaboration by CAD tools.

To solve these problems, researchers have focused their attention on the development of various solutions to improve the digitisation process and so the surface modelling result. The first common idea has moved in the direction of an adaptive digitising strategy. Following this idea the acquisition pitch should be varied in relation with the complexity of the object shape in order to avoid the presence of redundant punctual information located on non significant zones such as planes [4], shortening the digitisation time. All these approaches start from a first digitisation followed by the construction, under different parametric rules [5], of intermediate models. In

this way these methodologies allow to decide which are the zones that need to be re-digitised with a more precise strategies.

While the approaches proposed in literature need the construction of an intermediate model [6], in this work a different methodology, only based on a direct point cloud analysis, is developed.

2. Description of the new approach

The approach developed in this work starts with an initial raw acquisition of the surface points. In this first raw acquisition the proposed method localises the boundary of zones characterized by significant curvature. After this phase a second acquisition phase is conducted by employing larger pitches in areas with no significant morphological variations of the surface and by decreasing the dimension of pitches in the areas with significant changes in curvature. While the traditional approaches are usually based on the development of an intermediate mathematical model, and on the use of semi-automatic procedures to discriminate the zones that need to be deeply rescanned, the proposed approach operates directly on the measured point cloud by applying an automatic selective procedure.

2.1 Management of the measured points

The scanned points acquired in the first digitisation are reordered according to their associated *X-Z* and *Y-Z* planes, creating two different orders. This produces that, during the morphological analysis, the object surface is treated according to two orthogonal directions, the first along *X* axis and the second along *Y* axis. This kind of pre-processing phase allows a more simple management of points in the subsequent steps. In fact it permits to work in an ordered set of planes instead of a more complex three-dimensional space (Fig.1).

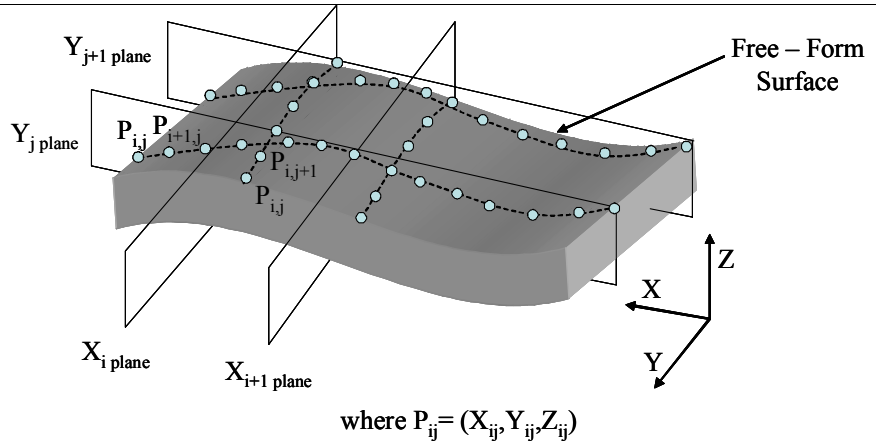

Figure 1: Management of measured points

2.2 Boundary definition

In this second step the algorithm allows to define the boundaries for the more accurate rescanning phase. The procedure is developed along X axis for all the planes individuated in correspondence of each Y value and along Y axis for all the planes individuated in correspondence of each X value [7].

The geometrical parameter used in the algorithm is the angle γ between two subsequent segments obtained by three successive points measured along the same axis, as, for example, given a plane j: $P_{i,j} \equiv (X_{i,j}, Y_{i,j,}$ $_{i,j})$, $P_{i+1,j} \equiv (X_{i+1,j}, Y_{i,j,}, Z_{i+1,j})$ and $P_{i+2,j} \equiv (X_{i+2,j}, Y_{i,j,} Z_{i+2,j})$ evaluated on X axis.

Referring to Fig. 2, if we define as $\alpha_{i,j}$ the inclination angle, with respect to the horizontal axis, of the first segment ($P_{i,j}$ - $P_{i+1,j}$) and as $\beta_{i+1,j}$ the inclination angle of the subsequent segment, $\gamma_{i,j}$ angle can be obtained by the difference:

$$\gamma_{i,j} = \beta_{i+1,j} - \alpha_{i,j} \tag{1}$$

$\alpha_{i,j}$ and $\beta_{i+1,j}$ angles can be evaluated as follows:

$$\alpha_{i,j} = arctg\left(\frac{Z_{i+1,j} - Z_{i,j}}{X_{i+1,j} - X_{i,j}}\right) \tag{2}$$

$$\beta_{i+1,j} = arctg\left(\frac{Z_{i+2,j} - Z_{i+1,j}}{X_{i+2,j} - X_{i+1,j}}\right) \tag{3}$$

Therefore $\gamma_{i,j}$ angle can be obtained by:

$$\gamma_{i,j} = arctg\left(\frac{Z_{i+2,j} - Z_{i+1,j}}{X_{i+2,j} - X_{i+1,j}}\right) - arctg\left(\frac{Z_{i+1,j} - Z_{i,j}}{X_{i+1,j} - X_{i,j}}\right) \tag{4}$$

From a nominal point of view, if $\gamma_{i,j}$ angle is zero it means that the three considered points make part of the same straight line in plane j. Hence there is no need of further measures between the three points for better evaluating the object curvature in that zone (Fig.2). It must be noted that this is true under the assumption of absence of sudden curvature variation between two subsequent points. This hypothesis is automatically verified when working with free-form surfaces and an adequate acquisition pitch.

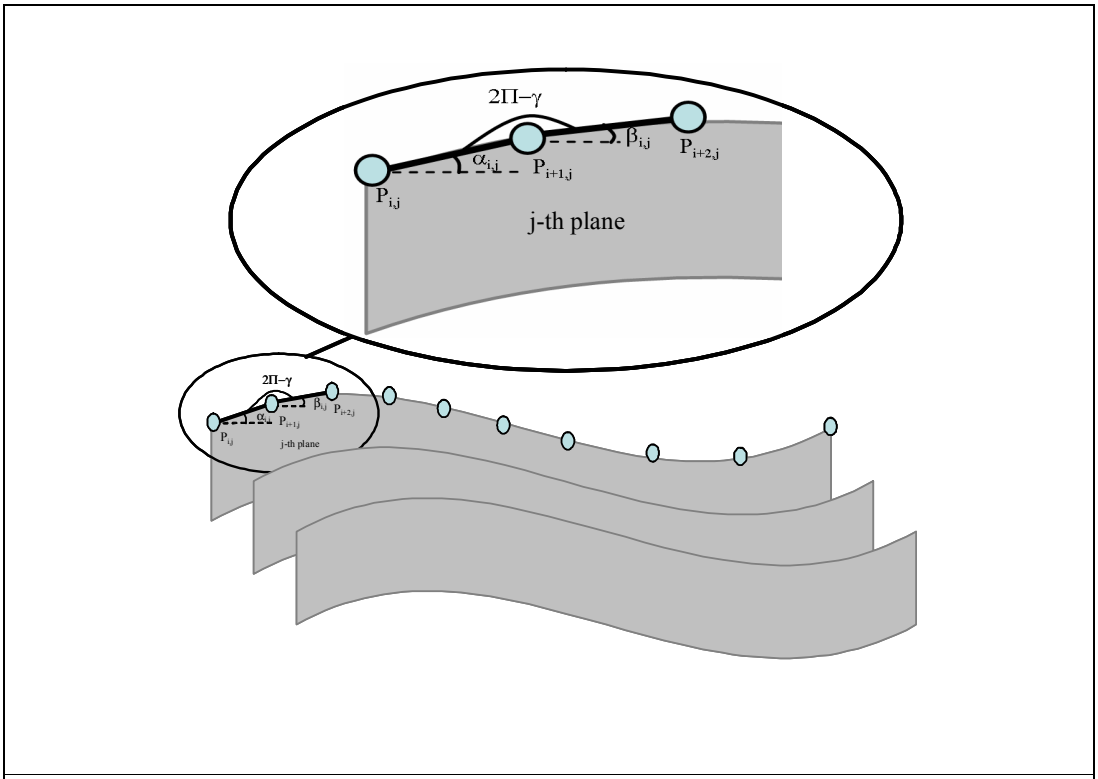

Figure 2: Geometrical parameter

Therefore, in order to give to the procedure a more strict coherence with the real behaviour of the measurement devices, it is necessary also to consider the presence of the measurement uncertainty.

$\gamma_{i,j}$ angle overall uncertainty can be evaluated starting from single point measurement uncertainties and utilising the following composition law [8]:

$$U(\gamma_{i,j}) = 2u(\gamma_{i,j}) = 2\sqrt{\sum_{l=1}^{N}\sum_{m=1}^{N}\frac{\partial\gamma_{i,j}}{\partial\xi_l}\frac{\partial\gamma_{i,j}}{\partial\xi_m}u(\xi_l,\xi_m)} = 2\sqrt{\sum_{l=1}^{N}\left(\frac{\partial\gamma_{i,j}}{\partial\xi_l}\right)^2 u^2(\xi_l) + 2\sum_{l=1}^{N-1}\sum_{m=l+1}^{N}\frac{\partial\gamma_{i,j}}{\partial\xi_l}\frac{\partial\gamma_{i,j}}{\partial\xi_m}u(\xi_l,\xi_m)} \quad (5)$$

where:

$\gamma_{i,j}$ is a function of $N = 6$ variables ξ_l ($\xi_1 \equiv X_{i+1,j}$, $\xi_2 \equiv X_{i,j}$, $\xi_3 \equiv X_{i+2,j}$, $\xi_4 \equiv Z_{i+1,j}$, $\xi_5 \equiv Z_{i,j}$, $\xi_6 \equiv Z_{i+2,j}$);

$U(\gamma_{i,j})$ is $\gamma_{i,j}$ extended uncertainty (expressed at 95% confidence level);

$u(\gamma_{i,j})$ is $\gamma_{i,j}$ standard deviation;

$u(\xi_l, \xi_m)$ is variable ξ_l and ξ_m covariance.

The correlation level between ξ_l and ξ_m is characterised by the correlation coefficient:

$$r(\xi_l,\xi_m) = \frac{u(\xi_l,\xi_m)}{u(\xi_l)u(\xi_m)} \quad (6)$$

where $r(\xi_l\ \xi_m) = r(\xi_m\ \xi_l)$ and $-1 < r(\xi_l\ \xi_m) < 1$. If ξ_l and ξ_m are independent, then $r(\xi_l\ \xi_m) = 0$, for every $l \neq m$. The covariance term of equation (5) can be written as a function of the correlation coefficient in the following way:

$$2\sum_{l=1}^{N-1}\sum_{m=i+1}^{N}\frac{\partial\gamma_{i,j}}{\partial\xi_l}\frac{\partial\gamma_{i,j}}{\partial\xi_m}u(\xi_l)u(\xi_m)r(\xi_m\xi_l) \tag{7}$$

Hence equation 5 becomes:

$$U(\gamma_{i,j}) = 2u(\gamma_{i,j}) = 2\sqrt{\sum_{l=1}^{N}\frac{\partial\gamma_{i,j}}{\partial\xi_l}u^2(\xi_l) + 2\sum_{l=1}^{N-1}\sum_{m=i+1}^{N}\frac{\partial\gamma_{i,j}}{\partial\xi_l}\frac{\partial\gamma_{i,j}}{\partial\xi_m}u(\xi_l)u(\xi_m)r(\xi_l\xi_m)} \tag{8}$$

If all the input variables are correlated with a correlation coefficient $r(\xi_l\ \xi_m) = 1$, the above equation becomes:

$$u^2(\gamma_{i,j}) = \left(\sum_{l=1}^{N}\frac{\partial\gamma_{i,j}}{\partial\xi_l}u(\xi_l)\right)^2 \tag{9}$$

Due to the fact that the points acquired on the surface are correlated, the standard deviation $u(\gamma_{i,j})$ of $\gamma_{i,j}$ angle along all the working planes is:

$$u(\gamma_{i,j}) = \left(\frac{\partial\gamma_{i,j}}{\partial Z_{i,j}}\right)\cdot u(Z_{i,j}) + \left(\frac{\partial\gamma_{i,j}}{\partial Z_{i+1,j}}\right)\cdot u(Z_{i+1,j}) + \left(\frac{\partial\gamma_{i,j}}{\partial Z_{i+2,j}}\right)\cdot u(Z_{i+2,j}) + \left(\frac{\partial\gamma_{i,j}}{\partial X_{i,j}}\right)\cdot u(X_{i,j}) + \left(\frac{\partial\gamma_{i,j}}{\partial X_{i+1,j}}\right)\cdot u(X_{i+1,j}) + \left(\frac{\partial\gamma_{i,j}}{\partial X_{i+2,j}}\right)\cdot u(X_{i+2,j}) \tag{10}$$

Given that the measurement uncertainty of the scanning device can be considered constant along the three Cartesian axes, it is possible to make some simplification on the mathematical formalisation above. For example, for the *j-th* plane:

$$u(Z_{i,j}) = u(Z_{i+1,j}) = u(Z_{i+2,j}) = u(X_{i,j}) = u(X_{i+1,j}) = u(X_{i+2,j}) = u_{const.} \tag{11}$$

and relation (10) becomes:

$$u(\gamma_{i,j}) = u_{const.}\cdot\left[\left(\frac{\partial\gamma_{i,j}}{\partial Z_{i,j}}\right) + \left(\frac{\partial\gamma_{i,j}}{\partial Z_{i+1,j}}\right) + \left(\frac{\partial\gamma_{i,j}}{\partial Z_{i+2,j}}\right) + \left(\frac{\partial\gamma_{i,j}}{\partial X_{i,j}}\right) + \left(\frac{\partial\gamma_{i,j}}{\partial X_{i+1,j}}\right) + \left(\frac{\partial\gamma_{i,j}}{\partial X_{i+2,j}}\right)\right] \tag{12}$$

The related overall uncertainty (at 95% confidence level) is (Fig.3):

$$U(\gamma_{i,j}) = 2\cdot u(\gamma_{i,j}) \tag{13}$$

As a consequence of this, we can individuate displacements of $\gamma_{i,j}$ angle from zero only if obtained values are external of the interval $\pm U(\gamma_{i,j})$ (Fig. 3).

3. Experimental validation

The entire procedure has been implemented in order to validate the efficiency of the approach. Working with Matlab the different functions, that characterise the method proposed, have been written in order to give to the algorithm a complete automation behaviour.

The flowchart (Fig.4), that shows only the main program structure, because the entire structure of the method would have been too extensive, collects the principals functions that implement the parameters and the equations shown in the paragraphs before.

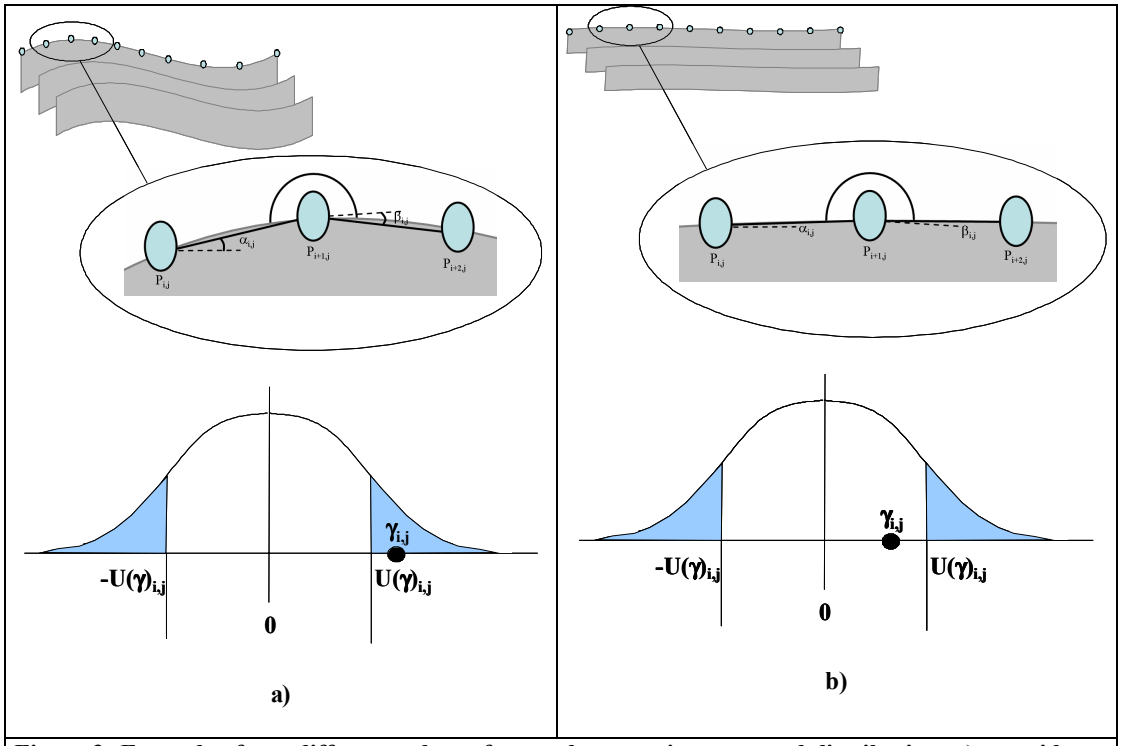

Figure 3: Example of two different values of $\gamma_{i,j}$ angle supposing a normal distribution: a) no evidence of curvature, b) evidence of curvature

Firstly the procedure manages the point cloud acquired with the 3D Scanner ("Distrib" function) indexing all the points in parallel planes and creating the new file "planes.txt". In the second stage loading the file "planes.txt" a first check is developed in order to see if the parallel planes collected are more than two or no. If the number of planes created is less then two, the algorithm could not work so the procedure is stopped, otherwise, if the number of planes is over than two, the procedure goes ahead creating a new data files, called "data.txt", that contains the coordinates of the boundary points of the different planes selected, the planes and points number. In the third stage the procedure, calling the function "Jump", evaluates which points are located in significant curvature regions employing the curvature evaluation parameter $\gamma_{i,j}$ and the $U(\gamma_{i,j})$ threshold, based on the punctual acquisition uncertainty. In the last step, calling the function "Interv", the algorithm, working on single planes, re-organizes the points selected with the "Jump" function, recording only the boundary points of the intervals characterised by successive points with significant curvature, and defines an interval starting and end point.

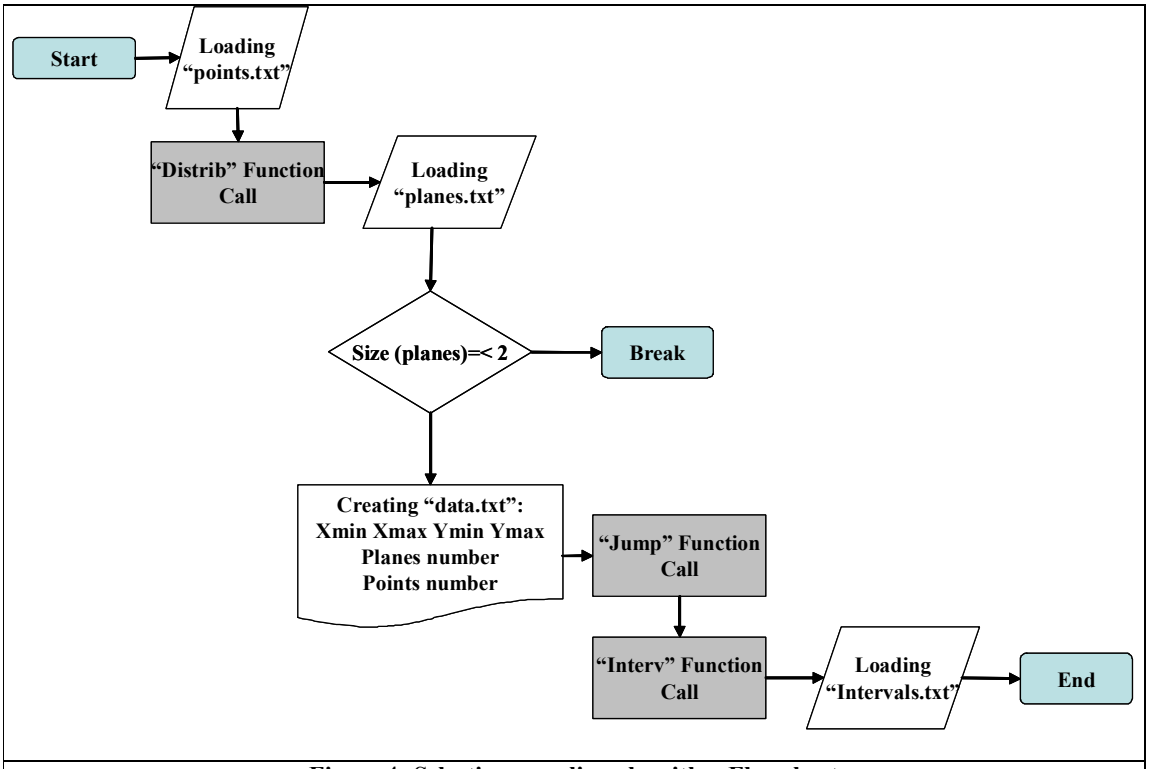

Figure 4: Selective sampling algorithm Flowchart

In order to verify the performances of the strategy proposed, the algorithm has been tested using an ideal geometry. The acquisition process has been simulated by generating sets of measurement points on different known surfaces (especifically a series of hemispheres with different curvature have been employed). This has been done in order to evaluate the sensitivity of the method in function of the measurement uncertainty and the surface curvature.

The simulation of the acquisition process has been performed by using the same scanning area for the different hemispheres. In particular, the used patch has been defined with a range between –10 mm and 10 mm (with respect to the centre of curvature) for X axes, and –10 mm and 0 mm for Y axes. The distance between two adjacent point, both along X axes and Y axes, was 1 mm (see Fig. 5).

After analyzing the results on a series of different simulation performed using hemispheres with curvature ranging from 0.1 mm^{-1} till 0.001 mm^{-1}, the test has confirmed that the sensibility of the method is directly correlated to the measurement uncertainty of the scanning device $u_{cost.}$: small values of uncertainty produce elevate sensibility. Considering, for example, the value $u_{cost.}$ = 0.025 mm, the method is able to discriminate a curvature larger than 0.01 mm^{-1}. This means that surfaces with curvature smaller or equal to 0.01 mm^{-1} will be confounded with a plane.

In a successive test a Gaussian perturbation has been introduced into the coordinate values of the simulated points, in order to simulate the variability due to the measurement uncertainty. The perturbation

amplitude has been imposed of the same entity of the uncertainty of a real measurement device ($u_{cost.}$ = 0.025 mm). The perturbed points and the results obtained with the application of the method are reported respectively in Fig. 6 and Fig. 7.

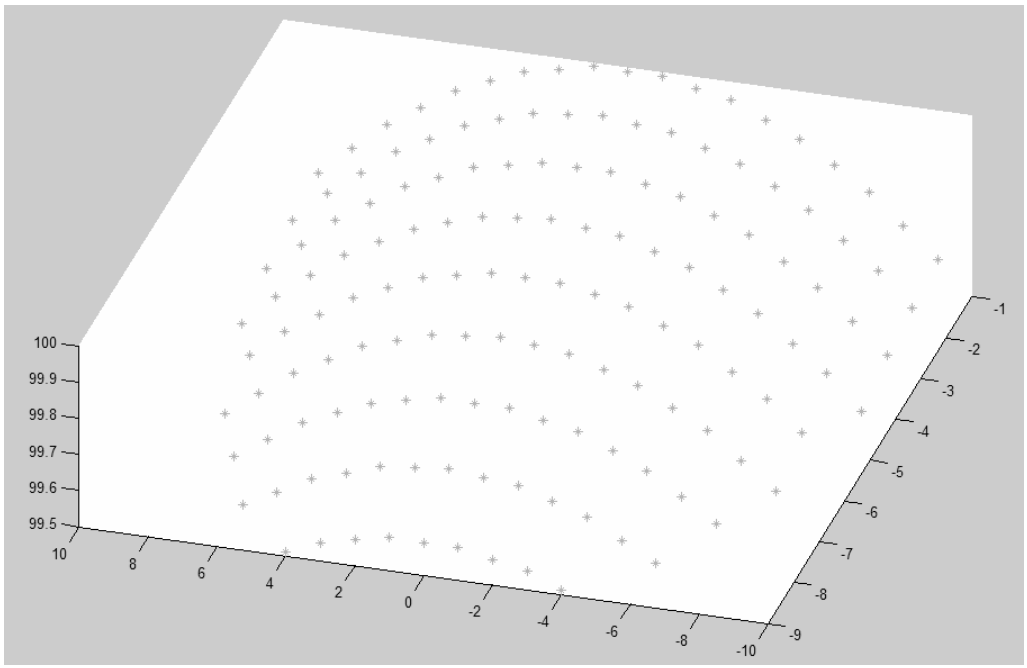

Figure 5: Testing sphere patch

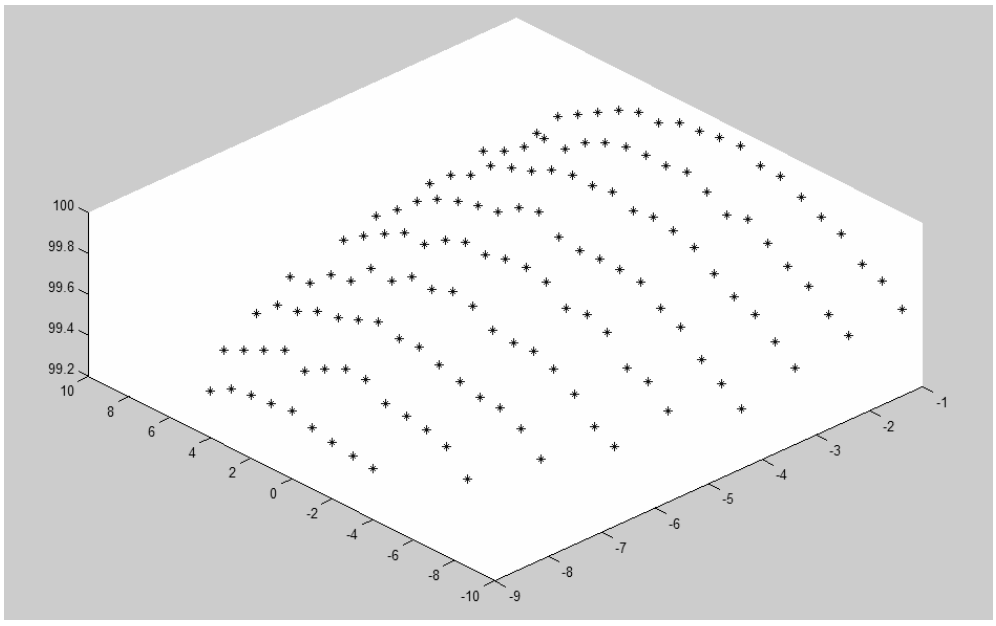

Figure 6: Testing sphere with noise

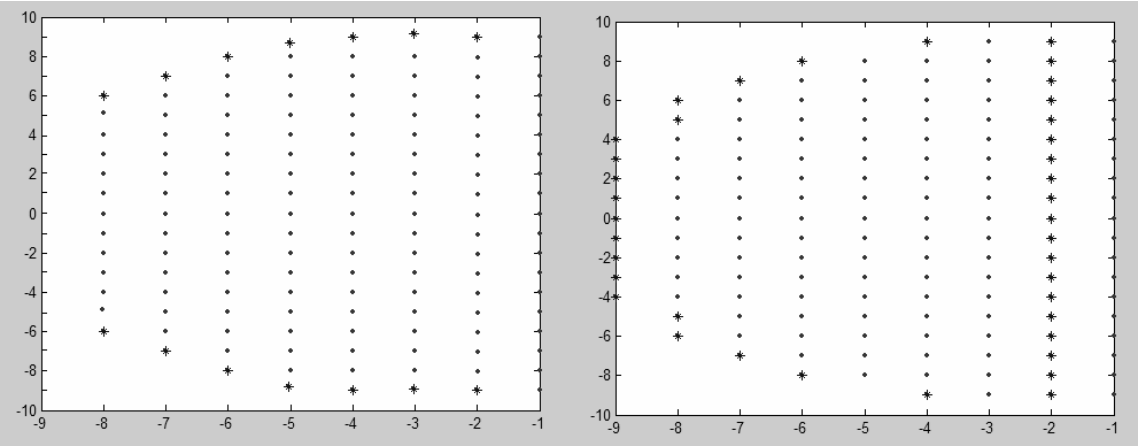

Figure 7: Area definition along *X* and *Y* planes. The boundaries (evidenced stars) localise the most significant curvature respectively in the *X* direction (a) and *Y* direction (b).

In a second phase, in order to develop an experimental validation of the procedure, a specific shape has been digitised with the use of a contact system, Roland Picza (Fig.8). The acquisition device employed for this work application is a contact system that employ a piezoelectric sensor for the digitalisation process. This system is composed by a head and a working table. The head is composed by a piezoelectric sensor connected with a little needle that is able to move outside from the head, along the z direction in order to touch the scanned surface. The head is also climbed on a guide that allows another degree of freedom along the x direction. The last movement is given to the working table that is able to translate along the y direction, with a maximum resolution value of 0,05 mm along x and y axis, for the grid acquisition.

Figure 8: 3D Scanner and digitalisation device

A effective sample, in term of free form surfaces, for the validation of the proposed methodology is a human face [9,10]. Looking at the morphology of the analysed surface (Fig. 9) it is easy to see that the most significant zones, in term of curvature, are the eyes, the mouth and the nose of the represented face. The other regions of the object does not show any significant morphological variations and can be considered non

significant zones. As a consequence, the algorithm should evidence those zones as the regions which need a deeper curvature analysis.

Figure 9: Human face

A first digitisation of the surface has been performed using a 1 mm x 1 mm pitch. Considering the specific scanner device uncertainty, as declared by the constructor, $U_S = 2 \cdot u_{cost} = 0.05$ mm, the overall uncertainty for every $\gamma_{i,j}$ angle can be calculated using equations 12 and 13. At this point the curvature analysis has been performed point by point using as discriminating threshold the obtained value for $U(\gamma_{i,j})$. Looking at the results (Fig. 10), it is possible to see a good level of coherence between the expected regions and the individuated zones with significant curvature.

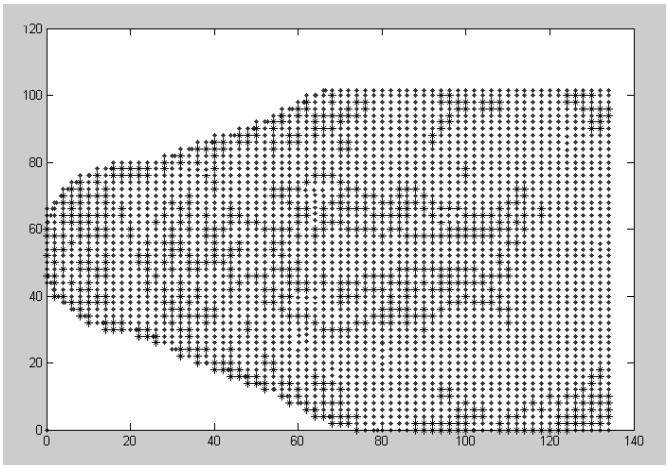

a)

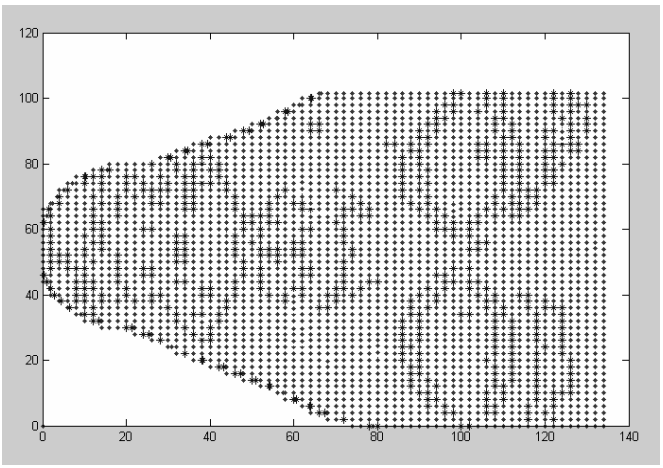

b)

Figure 10: Area definition: a) along *Y* planes, b) along *X* planes. The zones (evidenced stars) localise the most significant curvature variations respectively in the *X* and *Y* directions

In order to better understand the consistency of the analysis developed along X and Y axes, a merging of the boundaries obtained in these two directions is reported in Fig. 11.

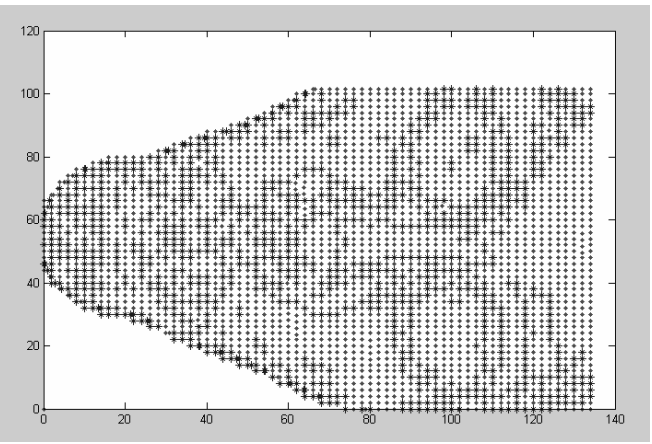

Figure 11: Area definition. Merging of curvature zones of Fig. 10.a and 10.b (evidenced stars).

In order to look at the sensibility of the model, a second experimental step has been run: the discriminating threshold has been forced to different values by imposing different values of the instrument uncertainty. A first result obtained with an uncertainty value of U_S = 0.04 mm (lower than the real one) gives rise to some unexpected zones which do not correspond to the real morphology of the sample surface (Fig. 12).

This behaviour is justified by the fact that the uncertainty of the instrument is higher than the used parameter and for that reason a great amount of measurement noise is caught.

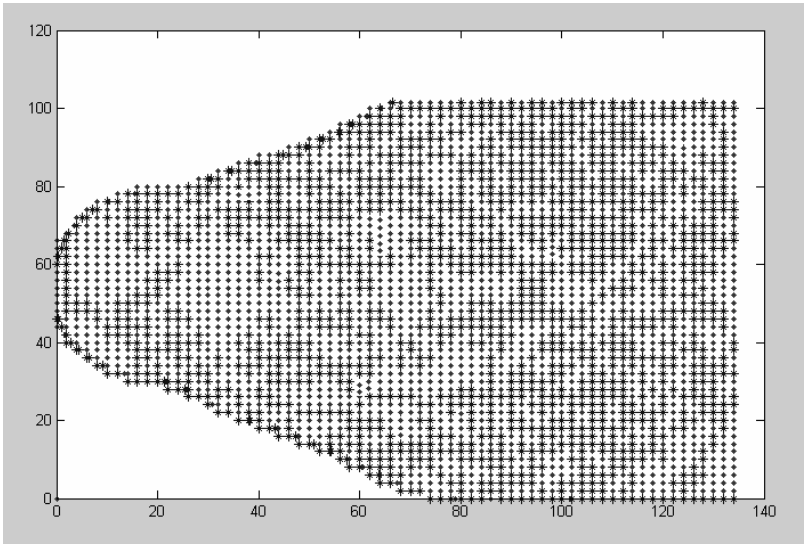

Figure 12: Wrong area definition.

A second result, obtained with an uncertainty value of U_S = 0.06 mm (higher than the real one), gives rise to significant resolution problems (Fig. 13).

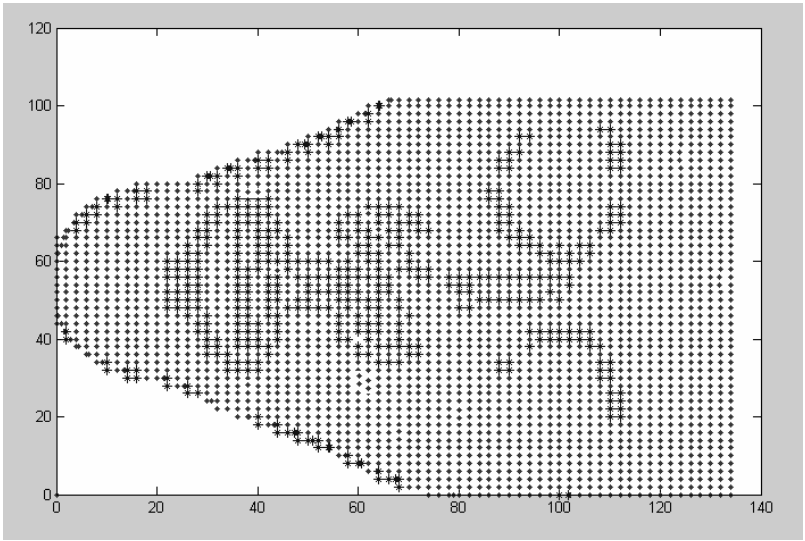

Figure 13: Wrong area definition

This could be shown by the absence of evidence over some zones in which a real curvature variation should be expected.

4. Conclusions

The paper describes an automatic procedure for selective identification of sampling points in reverse engineering applications. The aim is to individuate the boundaries of curvature zones, which need a further scansion and with a smaller dimension of pitches. The methodology is based on the curvature analysis of sample surface. The discrimination about curve zones is carried out by using the metrological characteristics of the inspection device. In particular, a threshold value for the inclination angle between two subsequent sampling intervals is defined on the basis of the inspection device measurement uncertainty.

The methodology has been applied to different kind of free-form patterns. Looking at the obtained results, it is possible to say that this procedure has a good level of applicability in automated scansion systems. In fact, the use of scanning device measurement uncertainty turns out a general purpose procedure for identification of critical zones without operator involvement and directly on the 3D scanner control unit.

The sensibility of the method depend on the first scanning pitch dimension, on the measurement system measurement uncertainty and on the smoothness of the tested surface. Experiments conducted with discrimination thresholds lower than that based on the measurement uncertainty show the appearance of

unexpected curvature zones, which do not correspond to the real morphology of the sample surface. On the other hand, higher threshold values produce the loss of some significant curvature zones.

The methodology described in this paper has been applied to a plane-by-plane bi-dimensional analysis of the scanned surface. The future work will be dedicated to a direct three-dimensional approach, and to the use of curvature variation instead of curvature only, trying to estimate also the pitch dimension in relation with the curvature value identified.

References

1. Bidanda B, Harding K., (1991) "Reverse Engineering: an Evaluation of prospective non contact technologies and applications in manufacturing systems", Int. J. Computer Integrated Manufacturing, Vol 30, No 10, pp.791 – 805.
2. Chen Y, Tang X., (1992) "Automatic digitisation of free-form curve by coordinate measuring machines", ASME.PED - Vol 62, Engineered Surfaces, pp.139 – 148.
3. Xi F., (1994) "Error compensation for the 3D line laser scanning data", International Journal of Advanced Manufacturing and Technology - Vol 32, pp.120 – 128.
4. Chen L., (1997) "An integrated reverse Engineering approach to reconstructing free – from surfaces, Computer Integrated manufacturing Systems", Vol.10, No 1, pp 49-60.
5. Iuliano, L., Vezzetti, E., (1999) "Comparison of Reverse Engineering Techniques for Jewellery Prototyping", AITEM (Associazione Italiana Tecnologia Meccanica), Brescia 1999, pp.231 -240.
6. S.Motavalli, (1991) "A part image reconstruction system for reverse engineering of design modifications", Journal of Manufacturing Systems, 10 (5), 383 – 395.
7. G.Farin, (1989) "Curvature and fairness of curves and surfacess", IEEE CGA, 9, 52 – 57.
8. BIPM, IEC, ISCC, ISO, IUPAC, IUPAP, OIML, (1993) "Guide to the Expression of Uncertainty in Measurement", ISO publication, Genève.
9. J.P.Moss, (1989) "A laser scanner system for the measurements of facial surface morphology", Journal of Optic and Lasers in Engineering, 10, 179- 190.
10. J.P..Moss, (1988) "Non contact measurement using a laser scanning probe", SPIE In process Optical Measurements 1012, 229- 239.